

Implementing Convolution Neural Network Model for Identifying and Detecting Waldenstroms Maculoglobulinemia Cancer

¹Nichenametla Rajesh, ²Vurukonda Naresh

Submitted:23/03/2023

Revised:27/05/2023

Accepted:11/06/2023

Abstract: This paper has aimed to design and implements a deep learning algorithm for identifying and detecting Waldenstrom Macroglobulinemia (WM) cancer. It affects the blood cells and causes various health problems in the human body. Several earlier research works have proposed clinical methods which can only be understood by medical experts and can not understand by non-medical candidates belonging to other related fields. Some of the researchers have used medical image processing methods for analyzing blood cell images for WM detection, where the accuracy is not satisfactory. This paper proposed a Convolution Neural Network model for analyzing and interpreting cell images for identifying and detecting WM cancer. Since the CNN learns the image deeply and extracts more features the prediction accuracy is high and it outperforms other methods. It provides F1-Score of 93.1% in WM prediction in detecting WM cancers from cell images.

Keywords: CNN, Cancer Analysis, Cell Images, Waldenstrom Macroglobulinemia, Blood Cells.

1. Introduction

IgM-secreting lymphoplasmacytic lymphoma is the classification given to the dormant B cell tumor known as Waldenström macroglobulinemia (WM) (R.G. Owen et al. (2003)). While approximately 20% of individuals may have the extramedullary disorder, the condition is mainly described by lymphoplasmacytic cell (LPC) penetration of the bone marrow (BM) (S.P. Treon, (2009)). It is a very rare kind of cancer that starts in white blood cells. The bone marrow of someone with WM excessively produces defective white blood cells, which flood out ideal blood cells. A protein that is produced by the defective white blood cells piles up in the bloodstream disrupts the flow and leads to problems. It is characterized as a specific variety of non-Hodgkin lymphoma. Losing weight, exhaustion, fever, headache, breathing difficulty, alterations in eyesight, anxiety, bleeding via the gums as well as nose, rapid bruises, etc. are some of the frequent symptoms of WM.

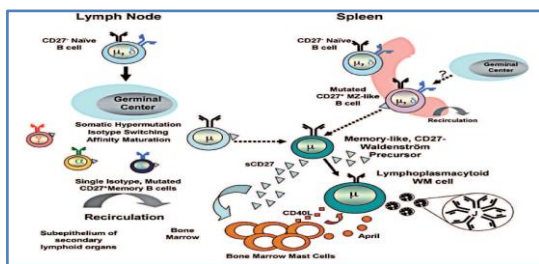


Fig 1. Extraction of Bone marrow cells

Patients with WM have migrating WM cells that may be detected by cytometry or clonotypic IgM V/D/J translocations, and their sickness load is correlated with these cells. Men and Caucasians having an average age of 60–70 years are more likely to have WM. Research has evaluated variations in WM individuals, and two possible alterations, notable mutations in the C-X-C chemokine receptor type 4 (CXCR4) and/or myeloid differentiation main reaction 88 (MYD88), have been identified (Z.R. Hunter et al. (2014)). Since MYD88 L265P is found in IgM MGUS, this somatic mutant may represent an initial malignant activity in the pathogenesis of WM/LPL which can be seen in Figure1. Unlike WM and IgM MGUS, additional IgM-secreting illnesses such as spleen peripheral region, nodal peripheral area, extranodal peripheral area lymphoma, and IgM-secreting numerous myelomas lack or rarely exhibit MYD88 L265P. The CXCR4 may be a secondary reason for the development of WM and their malignant clones. The CXCR4 mechanism is not fully understood in the WM patterns. However, its mutations are also a reason for the development of WM in patients. The CXCR4 is a type of G-protein coupled receptor that is the reason for lymphopoiesis. It also leads to cell trafficking caused by its ligand. The ligand is also called stromal cell-derived factor-1. The important pathways like RAS, Akt, and NF-KB are all activated using the SDF1/CXCR4. It is located in chromosome 2 at its long arm at position 21. It also helps to migrate and survive B lymphoid malignancies. Treon and his colleagues used Sanger sequencing to identify the CXCR4 mutations in 25% of the WM patients. In 7% of the people, the CXCR4

Koneru Lakshmaiah Education Foundation(KLEF)^{1,2}
nrjeshcse@kluniversity.in, naresh.vurukonda@kluniversity.in

C1013G mutations are recurrent mutations found. Apart from these mutations, other clonal mutations are not found in WM patients. It all depends on the mutated clone of MYD88. The CXCR4 mutations are seen in over 30% of the patients which is found using the qPCR by studying their mutations. In a study, over 98 WM patients the deep sequencing has helped to find the mutations of the CXCR4. It is done by deciphering the genomic landscape of CXCR4 from the single polymorphism nucleotide array.

Cell selection

Bone marrow samples are obtained from various patients who have WM. Immuno-magnetic beads are used to enrich the samples continued with Ficoll-paque gradient centrifugation. The marker combination are used to make a multi-parametric flow to detect the sample purity. In every case, over 90% of the light-chain isotype-positive B cells were detected.

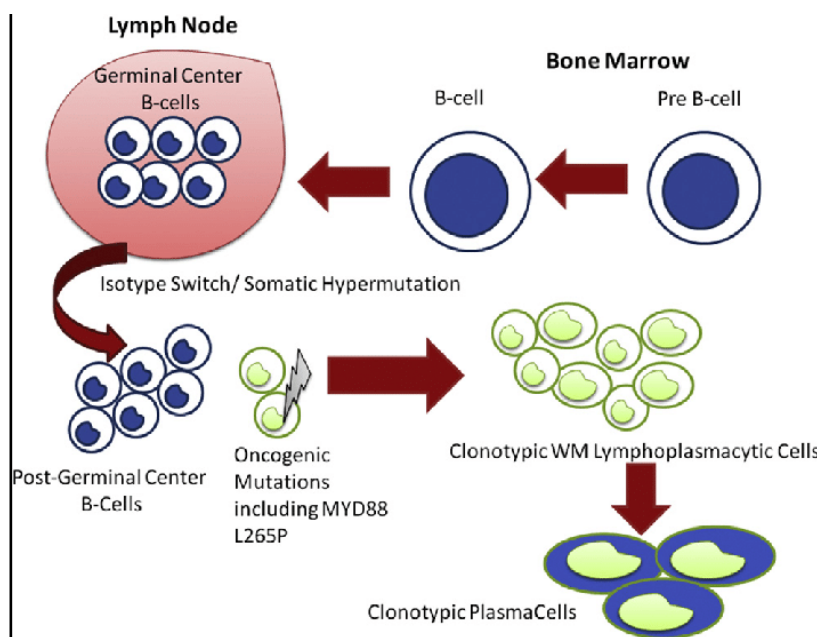


Fig 2. Cell selection process in WM patients

DNA sequencing

The Qui Amp kit is used to isolate the DNA from the cells. MYD88, L265P, CD79A, and CD79B were analyzed in the samples collected. PCR is used to amplify the C-terminal CXCR4 gene in the gDNA. Exons in the CXCR4 gene can be detected through the next-generation sequencing. The Ion Torrent PGM platform is used to analyze the NGS. The regions of interest in the DNA needs to be analyzed for which the amplicons that cover the region of interest needs to be measured. Mostly they range between 150 to 250 bp. The amplicon length of the libraries are maintained at 200-bp on a 318 chip. The torrent suite variant caller was used under the TS4.0 settings to perform the mutation calling. The mutated clone is verified variant allele frequency which is seen in Figure2. It counts the reads that are mapped to a specific position, which covers the variant base and also refer to the corresponding allele. It is then corrected using the tumor cells in B cell selected samples. Cells with more than 20 variants are considered positive. The CXCR4 sequence data is obtained through the mean depth coverage. Each coverage is done through the 2000x per nucleotide. NGS assay made a better

assessment in calculating the amount of CXCR4 mutant allele with 1% sensitivity.

Gene expression profiling

It is done by U133A arrays to the WM patients. TRIzol method is used to isolate the B-tumoral cells from the bone marrow region from which the total RNA is isolated. Multi-array Average algorithm is used to normalize the Expression data. With small number of replicates, the variance modeling can be improved by the Bioconductor R package that analyzes the differential gene expression. With a P value below 0.05 are considered to be expressed differentially. They are expressed in heatmap, in which the colors are represented as per the standard row values present in the input data. The GSEA analysis is done to many gene sets present with the C2 collection in MSigDB. The z score for the gene sets are calculated using the PGSEA package sets and the P value will be adjusted over multiple tests. The patterns obtained over multiple tests are collected and are fed into various machine learning algorithms that analyze the reliability of the patterns which is shown in Figure3.

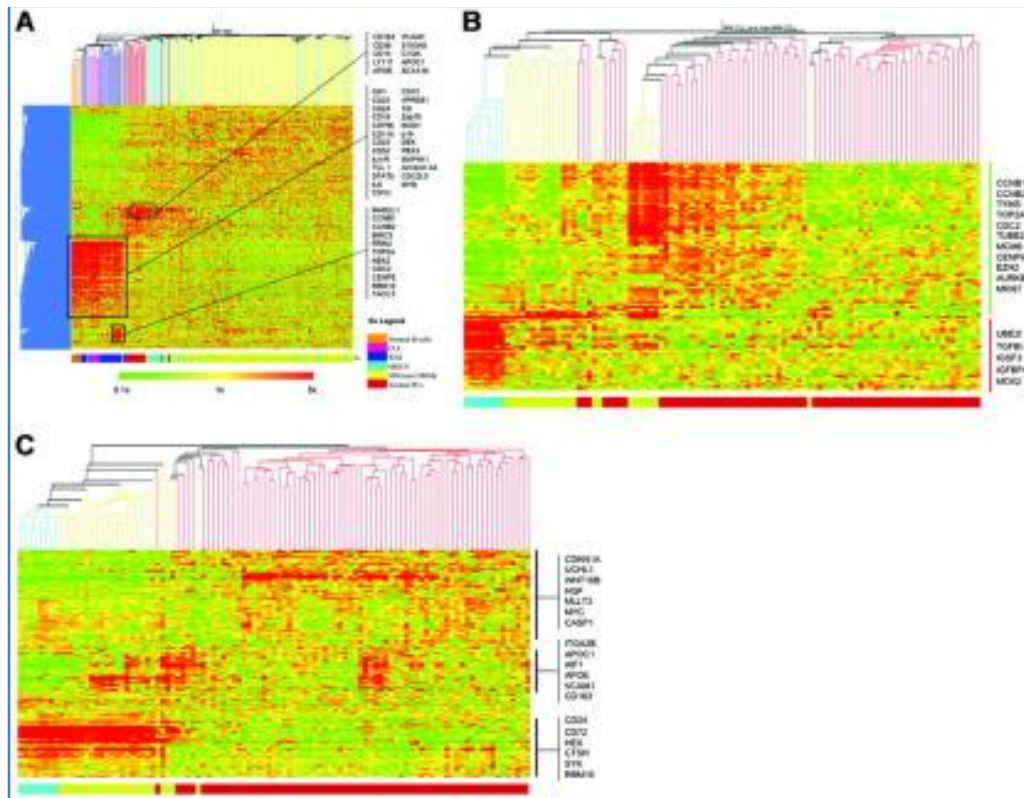


Fig 3. Gene profiling in the Waldenström macroglobulinemia

Machine learning and deep learning algorithms in WM Pattern recognition

Several machine learning algorithms are used in this testing. Generally, a standard pattern is fed into the machine learning models that learn about the patterns. Then these patterns are again compared with the patterns obtained and their reliability is checked. Usually for fast and efficient predictions classification algorithms are used. They classify the patterns into various types of bits that are similar to each other. Through this, the dimensions of the patterns are reduced. Then, the order of the divided patterns are noted. There may be different types of patterns however, the composition will be the same. The similarity between the patterns is studied by the machine learning algorithms and the same is seen in the testing samples. For such kind of tasks, usually classification algorithms are preferred. To usually consume less resources and also provide time efficiency. With the evolution of CXCR4 and MYD88, the number of patterns is numerous with mutations and these mutations amount to different types of DNAs responsible for WM. The recognition of WM patterns has become difficult through the classification algorithms. It is because; they become slow with large amount of data and also fail to understand the complexities in the patterns. To manage such complexities and to perform efficient classification of the WM patterns, deep learning algorithms may be considered. Deep learning algorithms consist of various layers that hold several information

which can be helpful in solving the complexities and also in providing efficient and accurate classification and prediction of WM patterns. The deep learning algorithm consists of several layers like convolutional, pooling and fully connected layers which will help in classifying the WM patterns.

2. Literature Review

An detailed overview of molecular biomarkers in WM and IgM-MGUS has been proposed by D. Drandi et al. (2022). The spectrum of IGM gammopathies includes WM, an indolent lymphoplasmacytic lymphoma that can range from asymptomatic to symptomatic and is distinguished by an excess of immunoglobulin M monoclonal protein. Cell-free nucleic acid biomarkers are currently being studied as a minimally invasive form of patient therapy. This work tries to overcome the present drawbacks and also a future guide for application in a precision medicine approach. H.Wang et al (2012) conducted a case study for analyzing data on WM in the United States. For data analysis and analysis of twenty-year data from the Surveillance, Epidemiology and End Results (SEER) programme, the study employed SEER*Stat. They claimed that little was known regarding the origin and prevalence of WM, a non-Hodgkin lymphoma (NHL) subtype in the US. The final findings revealed a substantial rise in the incidence of WM in whites aged 70 to 79 and in 3 geographic registry areas over the previous 20 years. However, over time,

the overall incidence of WM remained stable. According to R. Owen et al. (2003), WM is a rare lymphoproliferative illness. The condition, which exhibits IgM monoclonal gammopathy and bone marrow infiltration, must be viewed as a clinicopathological entity and not a clinical syndrome secondary to IgM secretion. Monoclonal IgM concentrations in WM might vary significantly. A concentration that can reliably distinguish WM from monoclonal gammopathy cannot be defined. WM can be identified on a bone marrow trephine biopsy in the presence of bone marrow infiltration, regardless of IgM content. The authors have also suggested straightforward criteria to distinguish between patients with symptomatic and asymptomatic WM.

S.Treon et al (2012) found in conducting a study on 135 patients with WM that familial predisposition was an important determinant of the outcome after treatment. They had first-or second-degree relatives with a B-cell lymphoproliferative disorder. They have also recommended studies to confirm the observations. R.Royer et al (2010) have analyzed large data on a mixture of MW patients unaffected relatives, sporadic patients, and non-familial patients. The examined clinical and environmental factors in a sample of WM families using a question in this instance. The information revealed that WM development was influenced by both genetic and environmental variables. They suggested well-planned case-controlled studies to support their recommendations. F. Nguyen-Khac et al (2013) a cytogenetic study on a series of 174 untreated patients with WM to find out the prognostic value which was not known in the earlier studies of this type. Also, the previous studies reported only a few recurrent chromosomal abnormalities. The researchers examined the prognostic value of chromosomal abnormalities in an international randomized trial. The researchers concluded that chromosomal abnormalities in conjunction with clinical and biological features could help with diagnosis and prognostication. E.Braggio et al. (2009) have aimed at characterizing the recurrent abnormalities associated with WM pathogenesis. For this, they have used an array-based comparative genomic hybridization approach. This was done to overcome the drawbacks of previous analyses that were historically limited in WM. The drawbacks were the difficulty in obtaining tumor metaphases and the non-availability of molecular consequences of the imbalances. They have concluded that the genetic consequences of the stated imbalances were elusive and further studies were required to clear molecular pathways and refine the search for them. In order to identify the early retinal abnormalities related to WM, M. Menke et al. (2006)

assessed patients with WM utilising indirect ophthalmoscopy with scleral depression, laser Doppler retinal blood flow measurements, and serum IgM and SV determination. With rising SV values, 46 WM patients showed far-peripheral haemorrhages and venous dilatation. In addition, the serum IgM and serum viscosity (SV) levels were to be determined by this study. The authors came to the conclusion that serum IgM and SV levels for the retinal symptoms of hyperviscosity syndrome were lower than those reported in other studies.

Waldenstrom Macroglobulinemia autologous and allogeneic transplant studies have been evaluated by M. Gertz et al. (2012). They believe that WM is a lymphoplasmacytic lymphoma that is particularly chemosensitive. When compared to those receiving stem cell transplants for multiple myeloma, there are more patients with this disease. In individuals with an indolent nature and favourable genetic profiles, Waldenstrom is an excellent disease for autologous stem cell transplant. Autologous transplants were efficient and underutilised in the management of the illness, according to the scientists' assessment. They have also said that allogeneic transplant should only be considered exploratory after all other chemotherapeutic treatments have been tried and in the context of a clinical trial. S.Sarosiek et al. (2021) have reviewed and summarized the adverse effects on treatment of WM and also the steps to decrease the risk of toxicity. Though, well-established treatment options for patients with WM are available the string of side effects during therapy cannot also be ruled out. To put in other words, multiple highly effective treatment options always come with a range of adverse effects. They have finally suggested that future researches should focus on patient safety without diminishing the effectiveness of treatment.

Convolutional Neural Networks

CNN is one of the widely used deep learning algorithm that uses multilayer perception to learn the complex features of the data. It is widely used in the image classification, facial detection, automation and robotics. In this paper, the CNN is initially trained with the WM samples to learn the features of the Human gene. It is used to recognize the WM patterns present in the samples. Then, new samples are sent to recognize the presence or absence of WM patterns. One of CNN's key advantages is its ability to infer local properties from samples, which enables it to recognise the samples' complicated aspects. Convolutional, pooling, and fully connected layers make up a CNN. The functioning of the CNN algorithm can be seen in the figure4.

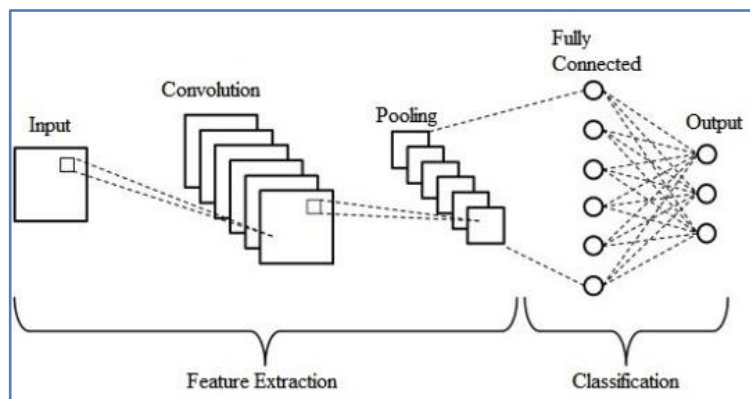


Fig-4. Architecture of the Convolutional Neural Networks

The convolutional layer consists of a many kernels that are used to determine the feature maps from the images. The kernels convolve the images into strides and convert their dimensions into integers and give them as output. After the striding process, there will be a decrease in the dimensions of the input images. To manage the decrease in the dimensions, 0 is added in the empty places. By adding zeros, the dimension of the images is maintained and it is called the zero padding. The convolutional layer processes the given images as per the following equation.

$$F_{i,j} = I * K_{i,j} = I_{i+m,j+n} * K_{m,n}$$

I stands for the input matrix, and K for the 2D filter with the $m \times n$ size. 2D feature map is referred to as F. The convolutional layer's operation is denoted by the symbol $I * K$. The feature maps' nonlinearity is raised through the application of Rectified Linear Nit (ReLU). The threshold input is maintained at zero.

$$f_x = \max(0, x)$$

The input dimension is down sampled using the pooling layer. By doing so, the number of parameters is decreased. The max pooling technique is the most popular one that extracts the greatest value from the input region. The convolutional and pooling layers extract features, which are then categorised by the fully connected layers.

Extended short-term memory

Recurrent neural networks (RNN) are better represented by this enhanced model. In consists of various memory blocks that helps to solve the gradient problems. The gradient problems are of two types, vanishing and exploding. It saves the long-term states after adding a cell state. LSTM is capable of relating the obtained information with the previously obtained data. The LSTM consists of three gates, they are, input forget and output. The input to the algorithm is x_t and C_t and C_{t-1} refer to the current and previous cell states. The h_t and h_{t-1} are the current and previous outputs. The LSTM architecture is shown in figure5.

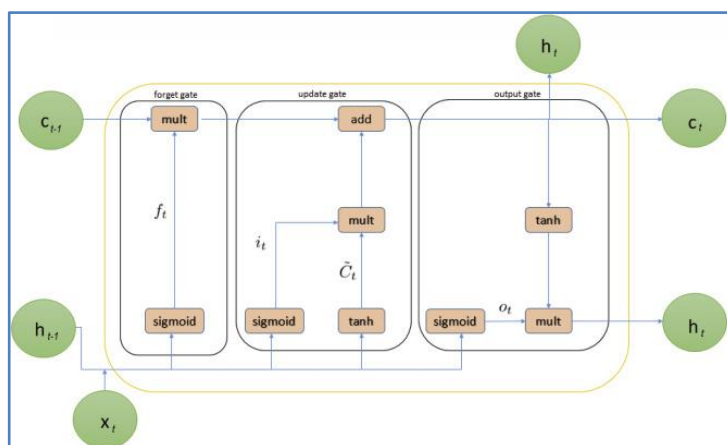


Fig -5 LSTM architecture

The movement of data through the LSTM architecture can be understood using the following equations,

$$i_t = \sigma(W_i \cdot h_{t-1} + x_t + b_i)$$

$$C_t = \tanh(W_c \cdot h_{t-1} + x_t + b_c)$$

$$C_t = f_t C_{t-1} + i_t C_t$$

Equation 3 demonstrates how the sigmoid layer is used to discover the significant sections by passing h_{t-1} and x_t through it. The extraction of new information following the transit of h_{t-1} and x_t via the tanh layer is seen in equation 4. The long-term information C_{t-1} and the current information C_t are merged to generate the

current information C_t . W_i represents the sigmoid output, and C_{tre} the tanh output.

Combined CNN-LSTM network

This paper combines both the CNN and LSTM algorithm to combine the WM patterns from the WM images. Both the architecture of CNN and LSTM are utilized to provide the maximum efficiency and accuracy. The LSTM method is used to classify the complex features that the CNN algorithm derives from the images. The hybrid network of the suggested method is depicted in figure 5. Convolution, pooling, and fully connected layers make up the network's 20 total layers, while the output layers are separated into 12, 5, 1, 1, and 1 groups. The softmax function is part of the output layer. Two to

three CNNs, one pooling layer, and a dropout layer with a 25% dropout rate make up each convolution block. The convolutional layers that extract features using ReLU function for activation have kernels with a 3x3 size. The Max-Pooling layer reduces the dimensions of the input image by reducing the kernel size to 2x2. The time information is extracted by the LSTM layer by transferring the function map to it. After convolution, the output shape is none, 7, 7, and 512. The dimension of the LSTM layer is 49,512 after the input size has been reshaped. The fully linked layer classifies the images using the time characteristics. Figure 6 displays the WM patterns that were discovered in the photos by this classification. The Table-1 displays the number of layers.

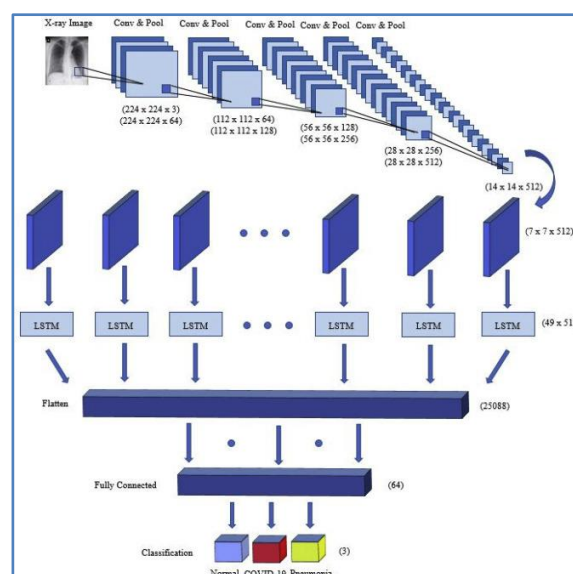


Fig 6. CNN-LSTM architecture

Metrics for evaluating performance

The measurements discussed to show how well the suggested algorithm performs. The images anticipated by the WM pattern are in TP. The normal cases that are identified as WM patterns are referred to as FP. The normal scenarios that the programme accurately detects are represented by the TN. The WM patterns that are identified as typical cases are designated as FN.

3. Experimental Results

The dataset is divided into training and testing halves in a 4:1 ratio. The generated outcomes go through a 5-fold

cross-validation process. The suggested algorithm's 12 convolutional layers have a learning rate of 0.0001. Experimental research determined that 125 epochs is the maximum number possible. The keras and tensorflow2 libraries of the Python programming language are used to implement the CNN-LSTM network. The hardware specifications are i7 7th generation, 16GB RAM, 1TB SSD and NVIDIA GTX 1650 GPU.

Table-1. Architecture and size of the CNN algorithm

Layer	Type	Kernel Size	Stride	Kernel	Input Size
1	Convolution2D	3 × 3	1	64	224 × 224 × 3
2	Convolution2D	3 × 3	1	64	224 × 224 × 64
3	Pool	2 × 2	2	–	224 × 224 × 64
4	Convolution2D	3 × 3	1	128	112 × 112 × 64
5	Convolution2D	3 × 3	1	128	112 × 112 × 128
6	Pool	2 × 2	2	–	112 × 112 × 128
7	Convolution2D	3 × 3	1	256	56 × 56 × 128
8	Convolution2D	3 × 3	1	256	56 × 56 × 256
9	Pool	2 × 2	2	–	56 × 56 × 256
10	Convolution2D	3 × 3	1	512	28 × 28 × 256
11	Convolution2D	3 × 3	1	512	28 × 28 × 512
12	Convolution2D	3 × 3	1	512	28 × 28 × 512
13	Pool	2 × 2	2	–	28 × 28 × 512
14	Convolution2D	3 × 3	1	512	14 × 14 × 512
15	Convolution2D	3 × 3	1	512	14 × 14 × 512
16	Convolution2D	3 × 3	1	512	14 × 14 × 512
17	Pool	2 × 2	2	–	14 × 14 × 512
18	LSTM	–	–	–	49 × 512
19	FC	–	–	64	25,088
20	Output	–	–	3	64

4. Result Analysis

Figure 6 displays the confusion matrix that was produced by the effectiveness of the suggested algorithms. The suggested CNN-LSTM incorrectly identified 1200 out of

the total 22283 WM images as normal images. For the normal photos, 1654 images were incorrectly labelled as WM images. It is clear that the suggested CNN-LSTM algorithm performs significantly better than existing conventional algorithms

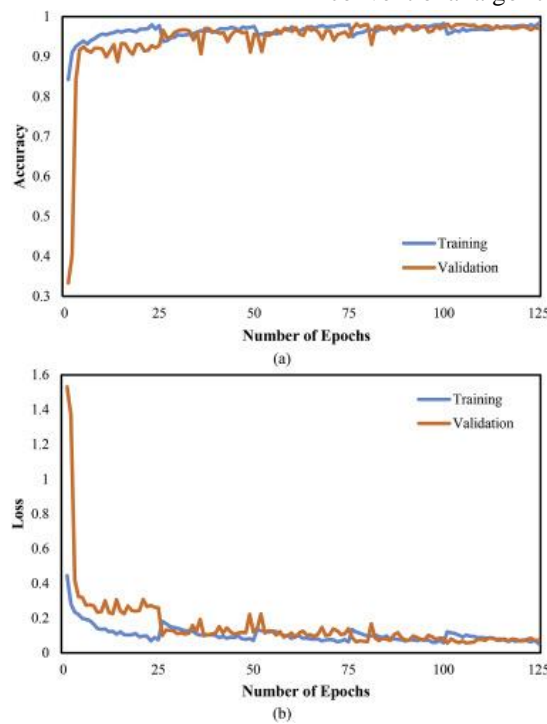


Fig 7. Evaluation metrics of the CNN-LSTM network

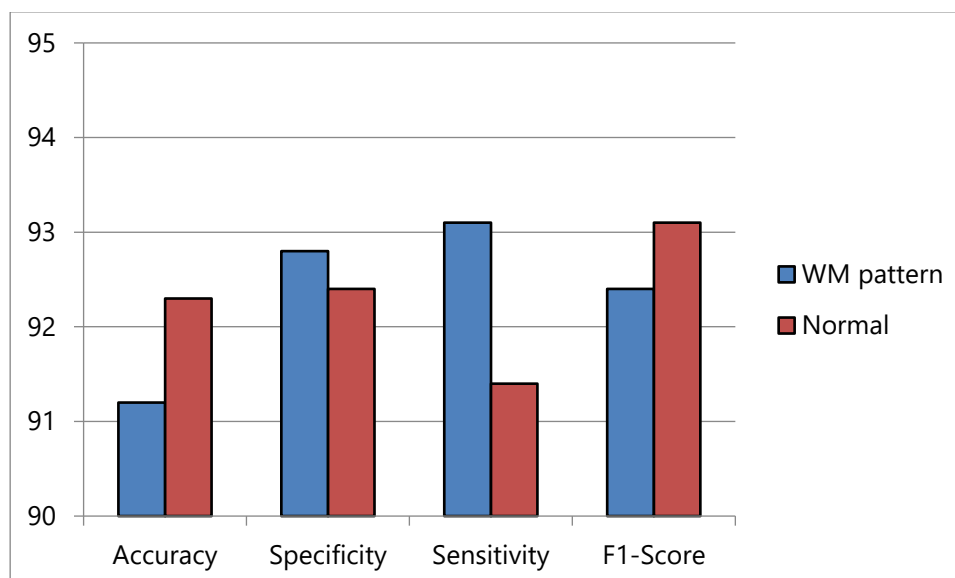


Fig 8. Evaluation metrics of the CNN-LSTM architecture

In the training and validation phases, the accuracy and cross-entropy of the proposed CNN-LSTM method performed as 91 and 92 across 125 epochs, respectively, in Figure 7. Losses for training and validation are 0.9 and 0.2, respectively. It is evident that the suggested algorithm offers superior cross-entropy and accuracy. Table 3 displays the total accuracy, sensitivity, specificity, and F1-score. The suggested algorithm has 92.8% specificity, 93.1% sensitivity, and 92.4% F1-score, as shown by the figure-8. Between the true positive and false positive rates is where the ROC curve is drawn. 92% of the ROC curve's area is under it. The proposed CNN-LSTM algorithm has an AUC of 92.9%, a Specificity of 92.8%, and an F1-Score of 93.1% according to the data.

5. Conclusion

The main objective of this paper is to increase the accuracy of WM cancer detection in blood cell images. Several earlier research works have proposed clinical methods which can only be understood by medical experts and can not understand by non-medical candidates belonging to other related fields. Some of the researchers have used medical image processing methods for analyzing blood cell images for WM detection, where the accuracy is not satisfactory. Compared to conventional methods, the accuracy of WM cancer detection needs to be improved. Thus this paper proposed a convolution neural network model for WM detection and classification. The experiment is carried out with Python and the results are verified. From the results, it is identified that the proposed CNN-LSTM provides F1-Score of 93.1% in WM prediction. In future work, a deep learning model needs to be implemented for analyzing genomic data to increase accuracy.

References

- [1] Owen, R. G., Treon, S. P., Al-Katib, A., Fonseca, R., Greipp, P. R., McMaster, M. L., ... & Dimopoulos, M. A. (2003, April). Clinicopathological definition of Waldenstrom's macroglobulinemia: consensus panel recommendations from the Second International Workshop on Waldenstrom's Macroglobulinemia. In *Seminars in oncology* (Vol. 30, No. 2, pp. 110-115). WB Saunders.
- [2] Treon, S. P. (2009). How I treat Waldenström macroglobulinemia. *Blood, The Journal of the American Society of Hematology*, 114(12), 2375-2385.
- [3] Hunter, Z. R., Xu, L., Yang, G., Zhou, Y., Liu, X., Cao, Y., ... & Treon, S. P. (2014). The genomic landscape of Waldenström macroglobulinemia is characterized by highly recurring MYD88 and WHIM-like CXCR4 mutations, and small somatic deletions associated with B-cell lymphomagenesis. *Blood, The Journal of the American Society of Hematology*, 123(11), 1637-1646.
- [4] Drandi, D., Decruyenaere, P., Ferrante, M., Offner, F., Vandesompele, J., & Ferrero, S. (2022). Nucleic Acid Biomarkers in Waldenström Macroglobulinemia and IgM-MGUS: Current Insights and Clinical Relevance. *Diagnostics*, 12(4), 969.
- [5] Wang, H., Chen, Y., Li, F., Delasalle, K., Wang, J., Alexanian, R., ... & Wang, M. (2012). Temporal and geographic variations of Waldenstrom macroglobulinemia incidence: a large population-based study. *Cancer*, 118(15), 3793-3800.
- [6] Owen, R. G., Treon, S. P., Al-Katib, A., Fonseca, R., Greipp, P. R., McMaster, M. L., ... & Dimopoulos, M. A. (2003, April).

- Clinicopathological definition of Waldenstrom's macroglobulinemia: consensus panel recommendations from the Second International Workshop on Waldenstrom's Macroglobulinemia. In *Seminars in oncology* (Vol. 30, No. 2, pp. 110-115). WB Saunders.
- [7] Naga Swetha, G. ., & M. Sandi, A. . (2023). A Brand-New, Area - Efficient Architecture for the FFT Algorithm Designed for Implementation of FPGAs. *International Journal on Recent and Innovation Trends in Computing and Communication*, 11(2), 114–122. <https://doi.org/10.17762/ijritcc.v11i2.6135>
- [8] Treon, S. P., Tripsas, C., Hanzis, C., Ioakimidis, L., Patterson, C. J., Manning, R. J., ... & Hunter, Z. R. (2012). Familial disease predisposition impacts treatment outcome in patients with Waldenström macroglobulinemia. *Clinical Lymphoma Myeloma and Leukemia*, 12(6), 433-437.
- [9] Royer, R. H., Koshiol, J., Giambarresi, T. R., Vasquez, L. G., Pfeiffer, R. M., & McMaster, M. L. (2010). Differential characteristics of Waldenström macroglobulinemia according to patterns of familial aggregation. *Blood, The Journal of the American Society of Hematology*, 115(22), 4464-4471.
- [10] Nguyen-Khac, F., Lambert, J., Chapiro, E., Grelier, A., Mould, S., Barin, C., ... & Leblond, V. (2013). Chromosomal aberrations and their prognostic value in a series of 174 untreated patients with Waldenström's macroglobulinemia. *Haematologica*, 98(4), 649.
- [11] Braggio, E., Keats, J. J., Leleu, X., Van Wier, S., Jimenez-Zepeda, V. H., Schop, R. F., ... & Fonseca, R. (2009). High-resolution genomic analysis in Waldenström's macroglobulinemia identifies disease-specific and common abnormalities with marginal zone lymphomas. *Clinical Lymphoma and Myeloma*, 9(1), 39-42.
- [12] Menke, M. N., Fekke, G. T., McMeel, J. W., Branagan, A., Hunter, Z., & Treon, S. P. (2006). Hyperviscosity-related retinopathy in Waldenström macroglobulinemia. *Archives of ophthalmology*, 124(11), 1601-1606.
- [13] Gertz, M. A., Reeder, C. B., Kyle, R. A., & Ansell, S. M. (2012). Stem cell transplant for Waldenström macroglobulinemia: an underutilized technique. *Bone Marrow Transplantation*, 47(9), 1147-1153.
- [14] Sarosiek, S., Treon, S. P., & Castillo, J. J. (2021). Reducing treatment toxicity in Waldenström macroglobulinemia. *Expert Opinion on Drug Safety*, 20(6), 669-676.
- [15] Gyawali, M. Y. P. ., Angurala, D. M. ., & Bala, D. M. . (2020). Cloud Blockchain Based Data Sharing by Secure Key Cryptographic Techniques with Internet of Things. *Research Journal of Computer Systems and Engineering*, 1(2), 07:12. Retrieved from <https://technicaljournals.org/RJCSE/index.php/journal/article/view/5>
- [16] Chng, W. J., Schop, R. F., Price-Troska, T., Ghobrial, I., Kay, N., Jelinek, D. F., & Bergsagel, P. L. (2006). Gene-expression profiling of Waldenstrom macroglobulinemia reveals a phenotype more similar to chronic lymphocytic leukemia than multiple myeloma. *Blood*, 108(8), 2755-2763.
- [17] <https://www.wjgnet.com/2307-8960/full/v8/i21/WJCC-8-5439-g002.htm> (results)